НАУЧНО-ТЕХНИЧЕСКИЙ ВЕСТНИК ИНФОРМАЦИОННЫХ ТЕХНОЛОГИЙ, МЕХАНИКИ И ОПТИКИ
сентябрь–октябрь 2022 Том 22 № 5 http://ntv.ifmo.ru/
SCIENTIFIC AND TECHNICAL JOURNAL OF INFORMATION TECHNOLOGIES, MECHANICS AND OPTICS
September–October 2022 Vol. 22 No 5 http://ntv.ifmo.ru/en/
ISSN 2226-1494 (print) ISSN 2500-0373 (online)

doi: 10.17586/2226-1494-2022-22-5-962-969

Ice reconnaissance data processing under low quality source images

Andrey V. Timofeev[1]✉, Denis I. Groznov[2]

[1,2] LLP "EqualiZoom", Astana, 010000, Kazakhstan

[1] timofeev.andrey@gmail.com✉, https://orcid.org/0000-0001-7212-5230
[2] d.i.groznov@yandex.ru, https://orcid.org/0000-0002-7874-7118

Abstract

A practically effective solution to the problem of automated processing of ice reconnaissance data in high latitudes is proposed. The intermediate result of ice reconnaissance is huge aerial survey data set consisting of images of low quality; this is a consequence of the difficult conditions of aerial survey in high latitudes. The goal of the study is to create a high-level method that can either efficiently process this pre-collected data set or perform real-time processing of similar images while ensuring high reliability in solving the problem of recognizing ice class distribution on the water surface with minimal computing resources. In particular, the problem of automatic classification of ice-floe size distribution (FSD) type for a three-class model based on aerial survey data is solved. The practically important case of low-quality images is considered, a common situation for the meteorological conditions of the Far North. The proposed approach is based on the use of machine learning methods, in particular on the well-known multi-class SVM (Support Vector Machine), which is extremely undemanding to computing resources and therefore can be implemented even by the onboard computer of an ice reconnaissance UAV. From the input images of low quality some numerical characteristics of the image are calculated which informatively characterize the image. These characteristics (features) are invariant to scaling, rotation and illumination as well as have a much smaller dimensionality than the original image. The main idea underlying the proposed method is to form an original set of features which are implemented in the original feature space. These features characterize large fragments of the analyzed image and are "stable", in contrast to the features that characterize small details. A new method of FSD type classification based on the processing of aerial survey data by using machine learning methods, which is sufficiently effective for processing low-quality images, has been proposed. Also, the original feature space for classification was proposed which ensured high practical efficiency of this method. The method has shown high efficiency when it is tested on a data set composed of low-quality real images (high blurriness, vagueness, presence of meteorological noises). The developed algorithm can be used for express analysis of ice reconnaissance data, including an ice reconnaissance UAV on-board software component.

Keywords

sea-ice floe size distribution, ice reconnaissance, image classification, multi-class SVM, image histogram, blurry images, sea-ice type classification

For citation: Timofeev A.V., Groznov D.I. Ice reconnaissance data processing under low quality source images. *Scientific and Technical Journal of Information Technologies, Mechanics and Optics*, 2022, vol. 22, no. 5, pp. 962–969. doi: 10.17586/2226-1494-2022-22-5-962-969

УДК 004.852

Обработка данных ледовой разведки при условии низкого качества исходных изображений

Андрей Владимирович Тимофеев[1]✉, Денис Игоревич Грознов[2]

[1,2] ТОО «Эквализум», Астана, 010000, Казахстан

[1] timofeev.andrey@gmail.com✉, https://orcid.org/0000-0001-7212-5230
[2] d.i.groznov@yandex.ru, https://orcid.org/0000-0002-7874-7118

Аннотация

Предмет исследования. Предложено практически эффективное решение задачи автоматизированной обработки данных ледовой разведки в высоких широтах. Промежуточный результат ледовой разведки — большой массив

данных аэрофотосъемки, состоящий из изображений низкого качества. Такой результат является следствием сложных условий аэрофотосъемки в высоких широтах. Цель работы — создание высокоэффективного метода, который при минимальных требованиях к вычислительным ресурсам способен или эффективно обработать предварительно собранный массив данных, или выполнить обработку подобных изображений в реальном масштабе времени. Метод должен обеспечить высокую надежность решения задачи по распознаванию класса распределения льдин на водной поверхности. Решена задача автоматической классификации типа распределения льдин по размерам для трехклассовой модели на основе данных аэрофотосъемки. Рассмотрен практически важный случай низкокачественных снимков, что является обычной ситуацией для метеорологических условий Крайнего Севера. **Метод.** Предложенный подход основан на использования методов машинного обучения, в частности на мультиклассовой машине опорных векторов, который является крайне нетребовательным к вычислительным ресурсам и поэтому может быть реализован даже бортовым вычислителем беспилотного летательного аппарата ледовой разведки. По входным изображениям низкого качества вычисляются многомерные числовые характеристики входного изображения, которые его информативно характеризуют. Характеристики (признаки) данного типа инвариантны к масштабу, повороту и освещению, а также имеют значительно меньшую размерность, чем исходное изображение. Основная идея, лежащая в основе предлагаемого метода, заключается в формировании оригинальной совокупности признаков. Признаки реализуются в оригинальном пространстве признаков, эффективно характеризуют крупные фрагменты анализируемого изображения и являются «устойчивыми», в отличие от признаков, характеризующих мелкие детали. **Основные результаты.** Предложен новый метод классификации типа распределения льдин на водной поверхности на основе обработки данных аэрофотосъемки с использованием методов машинного обучения, который эффективен для обработки низкокачественных изображений бортовым вычислителем беспилотного летательного аппарата ледовой разведки. Предложено оригинальное пространство признаков классификации, которое обеспечивает высокую практическую эффективность данного метода. Метод показал высокую эффективность при тестировании на наборе данных, составленном из реальных изображений низкого качества (высокая размытость, нечеткость, наличие метеорологических помех). **Практическая значимость.** Разработанный алгоритм может быть использован для экспресс-анализа данных ледовой разведки, в том числе и как компонент программного обеспечения бортовых вычислителей беспилотных летательных аппаратов ледовой разведки.

Ключевые слова

распределение размеров льдин, ледовая разведка, классификация изображений, мультиклассовая SVM, гистограмма изображения, размытые изображения, классификация типов морского льда

Ссылка для цитирования: Тимофеев А.В., Грознов Д.И. Обработка данных ледовой разведки при условии низкого качества исходных изображений // Научно-технический вестник информационных технологий, механики и оптики. 2022. Т. 22, № 5. С. 962–969 (на англ. яз.). doi: 10.17586/2226-1494-2022-22-5-962-969

Introduction

Shipping routes in the Northern latitudes, including the Northern Sea Route, do not have a permanent geographical reference and are formed based on a set of hydro-meteorological information which comes to the ship. As a rule, the total length of the route, in this case, is a variable value since throughout the route the vessel is under the influence of various ice conditions. In this case, the tortuosity coefficient always exceeds unity, and additional route length increase in old ice due to their circumvention is 10–30 % [1]. When laying routes in the Northern latitudes, the concept of a rational route that best meets some formal criterion (for example: route length, travel time along the route, fuel economy and others) plays an important role [2]. The main criterion used when constructing a rational route in the Northern latitudes is the total time spent on its passage time. A rational route is usually laid through the zones where: total ice cohesion is minimal, young ice forms prevail, and ice torsion is minimal. All this information can be obtained operatively only from ice reconnaissance data. Thus, without taking into account hydro-meteorological information, which is mainly the result of ice reconnaissance, the construction of a rational route is fundamentally impossible. Therefore, the role of ice reconnaissance in the set of tasks for providing logistics in northern latitudes is extremely important. The main navigational characteristic to be monitored during ice reconnaissance is the "ice cohesion" characteristic. Ice cohesion is the ratio of the area of ice in area X to the total area of this area expressed in fractions or scores [3]. Let us denote this parameter by the symbol $S(X)$. It is the parameter $S(X)$ that cardinally affects the ability to navigate in a particular area of the sea [3]. More precisely: the resistance of broken ice increases in proportion to the value of $(2 - S(X))S^2(X)$ [3]. Somewhat different, but close in meaning, ice cohesion can be described by the concept of "floe size distribution" (FSD) [4]. There are many papers devoted to the study of FSD, e.g., [4–11], from which follows that this FSD is well approximated by the power law. At the same time, some works consider more complex models, such as mix of power law and Gaussian law or the mix of two power laws with different parameters. Depending on the type of FSD, the ice is classified into classes according to the N point system. That is, solid ice gets the maximum number of points (N), and sparse ice gets the minimum number of points. Different applications of the FSD concept imply different values of N. For example, in [12] $N = 10$, and in [4] $N = 3$. From a practical point of view, it is the ice cohesion score assigned to a particular area Ξ_i of the sea surface with an ice cohesion value $S[\Xi_i]$ that is important. Let's denote this value by γ_i, $\gamma_i = \{1, \dots N\}$. In practice, the value of γ_i is calculated using the processing (manual or automatic) of some image $I(\Xi_i)$ of the surface area Ξ_i. The image $I(\Xi_i)$ can be made in one or another spectral range, this image can be obtained by one or another means of aerial photography. The data processing procedure D, which calculates the value γ_i based on $I(\Xi_i)$,

in fact, maps the set of all possible images of different parts of the sea surface (which form the set Ξ) onto the set $\{1, \dots N\}$. That is:

$$\Xi \xrightarrow{D} \{1, \dots N\}.$$

$$\gamma = D(I(\Xi_i)) \in \{1, \dots, N\}, I(\Xi_i) \in \Xi.$$

In fact, D is a classifier. Depending on the value of γ_i, the decision is made to include or not to include the section Ξ_i in the ship's route. It follows from the definition that γ_i is a discrete (otherwise coarse) descriptor of the value $S[\Xi_i]$.

The efficiency of D classifier implementation directly affects the correctness of determining the value of γ, and consequently, the efficiency of ice reconnaissance data implementation. Many works are devoted to methods of construction of the classifier D, for example [13–25]. Different methods of image processing are traditionally used, but the main accent is made on studying the boundaries of elements of a scene which represents an image. In this direction, considerable progress has been made including the use of the fashionable concept of Deep Learning [19]. In this work, Deep Convolutional Neural Network is successfully used to process ice reconnaissance data.

Against the background of huge recent achievements in the field of ice reconnaissance data, it remains a problem to construct such a classifier D which would be able to work with images of very low quality. Namely, low-quality ice images are not uncommon when operating in the High Latitudes using UAVs equipped with visible range sensors due to the chronically difficult weather conditions of this region. The images that are practically used to determine γ are often very blurry and highly noisy. As a rule, traditional image processing methods based on the analysis of image element boundaries (in fact: local contrast gradients and hessians) proved to be ineffective when processing blurred images [26]. In addition, developers are often faced with the problem of a training corpus of small volume. Also relevant is the task of ensuring the processing of ice reconnaissance data directly on board the UAV which imposes additional requirements for optimizing the computational complexity of the algorithms for determining γ. Therefore, the main goal of this paper is to develop a classifier D that would be operable for low-quality image processing, will remain operable for training on a small volume image body, and will be adaptable for implementation in the onboard complex of a small UAV.

Materials and Method

Description of the Features Space used

For automatic classification of images, explicitly or implicitly, some numerical characteristics of the image are calculated informatively characterizing the image. Ideally, they are invariant to scaling, rotation and illumination, and also have a significantly smaller dimensionality than the original image. These characteristics are called features. Typical examples of features are: histograms, image pixel intensity, contrast gradient, contrast hessian, SIFT-descriptors (spatial histogram of the image gradients), HOG (histogram of oriented gradients) and so on. The main idea underlying the proposed method is to form such features that characterize large fragments of the analyzed image, avoiding the use of features that characterize small details. We will call the feature of the first type — global and the feature of the second type — local. The main task of ice reconnaissance is to estimate the FSD type for quite large fragments of sea surface. This problem can be solved by different methods that allow you to use both global and local features. For example, in [8, 11, 21] both types of features are considered, and in [4, 19, 24] preference is given to the study of local features. For the case of blurred, noisy images considered in this paper, the use of fine details of the image, for example, based on the calculation of contrast gradients and hessians, is problematic. In other words, in this case, computing local features involve unacceptable errors. Local features computed in this way are uninformative and therefore unsuitable for solving the problem of FSD classification or other concepts characterizing FSD, in particular, for determining the parameter γ. On the other hand, global features are less dependent on the parameters of image blurring (although such dependence exists). The stability of global features is largely determined by the correlation radius of the image: the larger this value is, the more stable the global features are to the effects of blurring and noisiness factor. That is why this paper focuses on the use of global features. Initially, a fairly wide set of features was considered: more than thirty. At subsequent stages, this set was reasonably narrowed down by selecting the most informative features. Several methods were used including three so-called "filtering" methods: chi-square, Pearson correlation and analysis of variance (ANOVA), as well as adaptive method of backward elimination. As a result, the following set of features was obtained:

$$f_\Xi = (\mathbf{E}[I(\Xi)], |\Xi|, ST[I(\Xi)], H_m[I(\Xi)], r_\Xi, E(A_\Xi|x \geq r_\Xi), st(A_\Xi|x \geq r_\Xi)).$$

Here

$I(\Xi) = \{i_x | x \in X_{i(\Xi)}\}$ is image of Ξ, x-coordinates; $X_{I(\Xi)}$ is image $I(\Xi)$ coordinate set; and i_x is intensity in image point with coordinates x;

$\mathbf{E}[I(\Xi)] = \sum\limits_{x \in X_{I(\Xi)}} i_x |X_{i(\Xi)} I^{-1}$, hereinafter, the entry $|B|$ denotes the power of the set B;

$|I(\Xi)| = \max\limits_{x \in X_{I(\Xi)}} (i_x) - \min\limits_{x \in X_{I(\Xi)}} (i_x)$;

$ST(\Xi) = \sqrt{\sum\limits_{x \in X_{I(\Xi)}} (i_x - \mathbf{E}[I(\Xi)])^2 |X_{I(\Xi)}|^{-1}}$;

$H_m(\Xi)$ is histogram of $I(\Xi)$ with m bins;

$A_\Xi(l)$ is autocorrelation function of the $I(\Xi)$ (averaged over different slices), $l \in (0, d)$ — pixel shift; d is determined by the size of the $I(\Xi)$;

r_Ξ is correlation radius of the image (averaged over different slices);

$E(A_\Xi(l)|l \in (r_\Xi, d)) = \sum\limits_{l \geq r_\Xi} A_\Xi(l)(d - r_\Xi)^{-1}$;

$st(A_\Xi|x \geq r_\Xi) =$

$$= \sqrt{\sum_{l \geq r_\Xi} A_\Xi(l) - E(A_\Xi(l)|l \geq r_\Xi))^2 ((d - r_\Xi)(d - r_\Xi - 1))^{-1}}.$$

In numerical studies it was assumed that $m = 14$. The features f_{Ξ} are defined in the corresponding feature space **F**, consisting of real vectors of length 20.

Description of the Data Set used

To set up and test the proposed classifier, we used a Data Set specially created for this purpose. This Data Set included, according to the classification from [4], images of three FSD distribution classes, namely: "Pack Ice", "Marginal Ice Zone" and "Open Ocean" (Fig. 1). When setting up the problem, the use case of so-called "background" class has been deliberately excluded. Images of all three classes were collected from open sources. Then, in order to simulate the influence of a complex meteorological situation, the images were subjected to the procedure of artificial noising by spatially correlated noise and smoothing by a Gaussian filter.

Data Set was obtained, in which class PI ("Pack Ice") corresponds to 96 samples, class MIZ ("Marginal Ice Zone") corresponds to 76 samples, class OO ("Open Ocean") corresponds to 192 samples. Fig. 2 shows information about the class "Open Ocean". Fig. 3 shows information about the class "Marginal Ice Zone", and Fig. 4 shows information about the class "Pack Ice". It can be seen from the figures that the video material is of very low quality: ice edges are very blurred, contrast is low. But it is images of such quality that are typical when using small UAVs in the difficult meteorological conditions of the High Latitudes.

Description of the *D*-classificator used

In practice, the amount of power available to developers and researchers for training Data Set with aerial survey data is affected by legal restrictions. In particular, special licenses are usually required to use high-resolution remote sensing data. A significant number of modern airborne video sensors fall under this limitation. Thus, the Data Set with aerial imagery data available to a particular developer-researcher may by no means always be of significant (more than a thousand samples per class) power. In the present work, we assume that for training classifier *D* researchers have access to a Data Set of relatively small power. Since the dimensionality of feature space is relatively small, and the images in Data Set have a relatively large correlation radius (8 or more pixels), the samples of the same class will relatively "smoothly" differ from each other by the metric of **F**-space. Under these conditions, it is logical to use a conventional and very computationally economical Multi-Class Support Vector Machine (MC-SVM) as a *D*-classifier [27]. For comparison, a DL-classifier was also used in ResNet20 [28]. During training, in order to ensure control of the generalization ability of the classifiers, the standard Cross Validation scheme was used, in the LOO (leave-one-out) variant. For the MC SVM classifier, given the multiclass formulation of the problem, a one-vs-rest strategy was used.

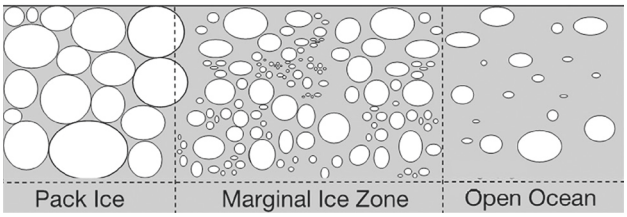

Fig. 1. FSD types used in this study. This figure is taken from the article [4]

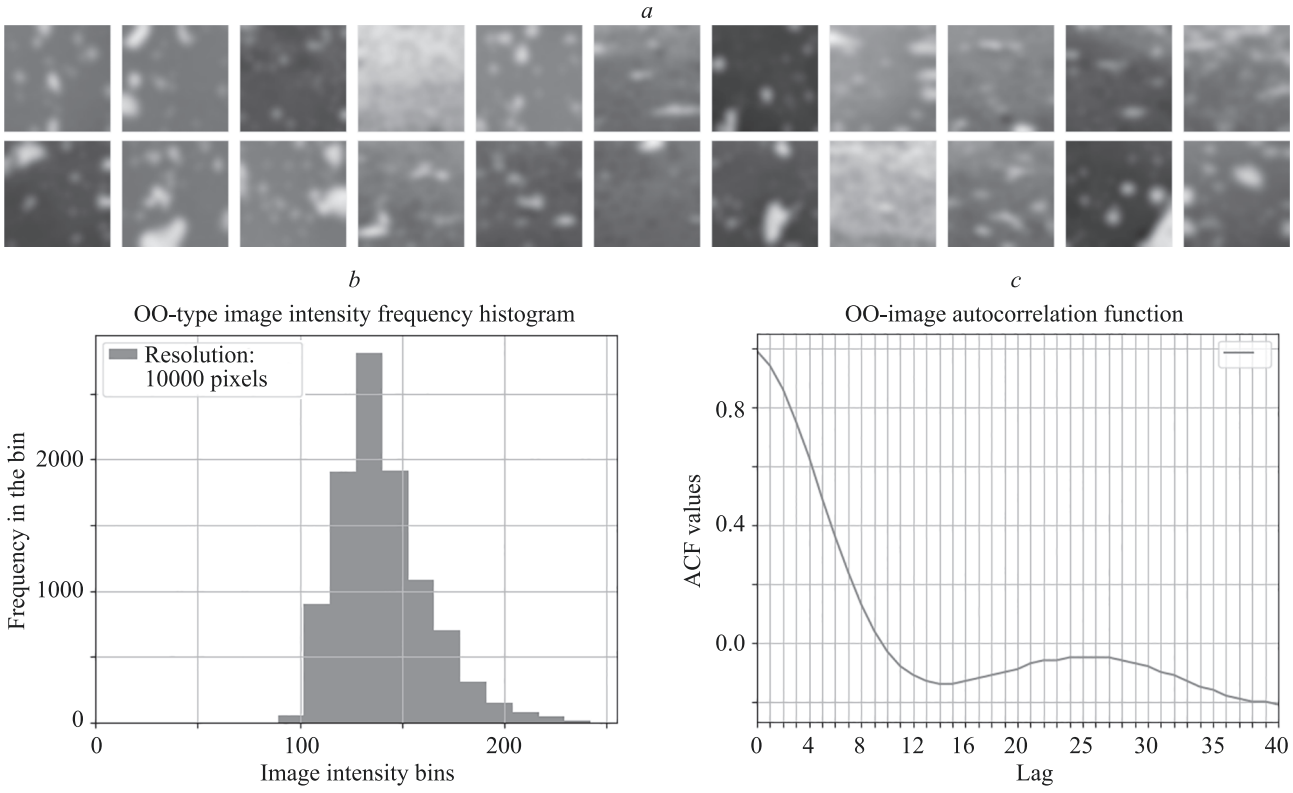

Fig. 2. Class "Open Ocean" (OO). Typical sample images from the OO-class (*a*). Intensity histogram plotted over the entire typical image from the OO-class (*b*). Typical autocorrelation function of an OO-image (averaged over different slices) (*c*)

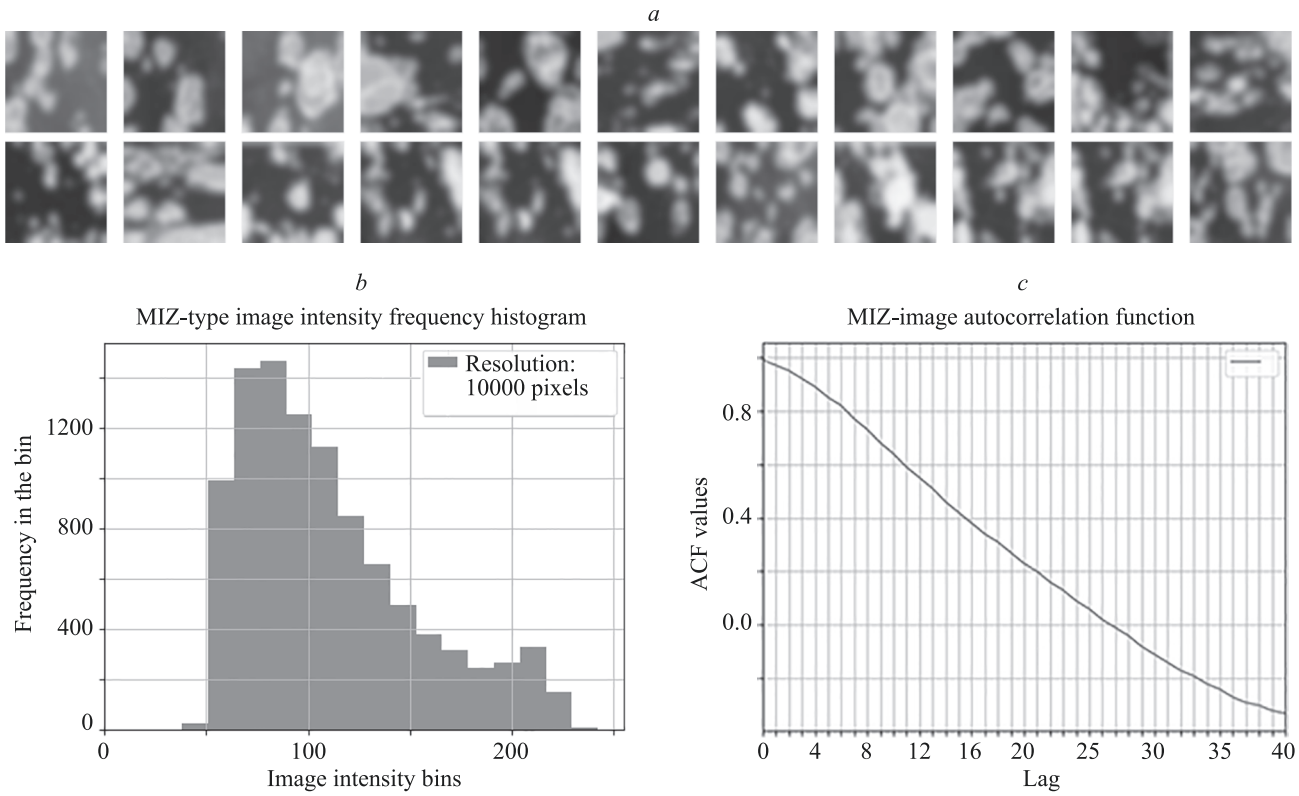

Fig. 3. Class “Marginal Ice Zone” (MIZ). Typical sample images from the MIZ-class (*a*). Intensity histogram plotted over the entire typical image from the MIZ-class (*b*). Typical autocorrelation function of MIZ-image (averaged over different slices) (*c*)

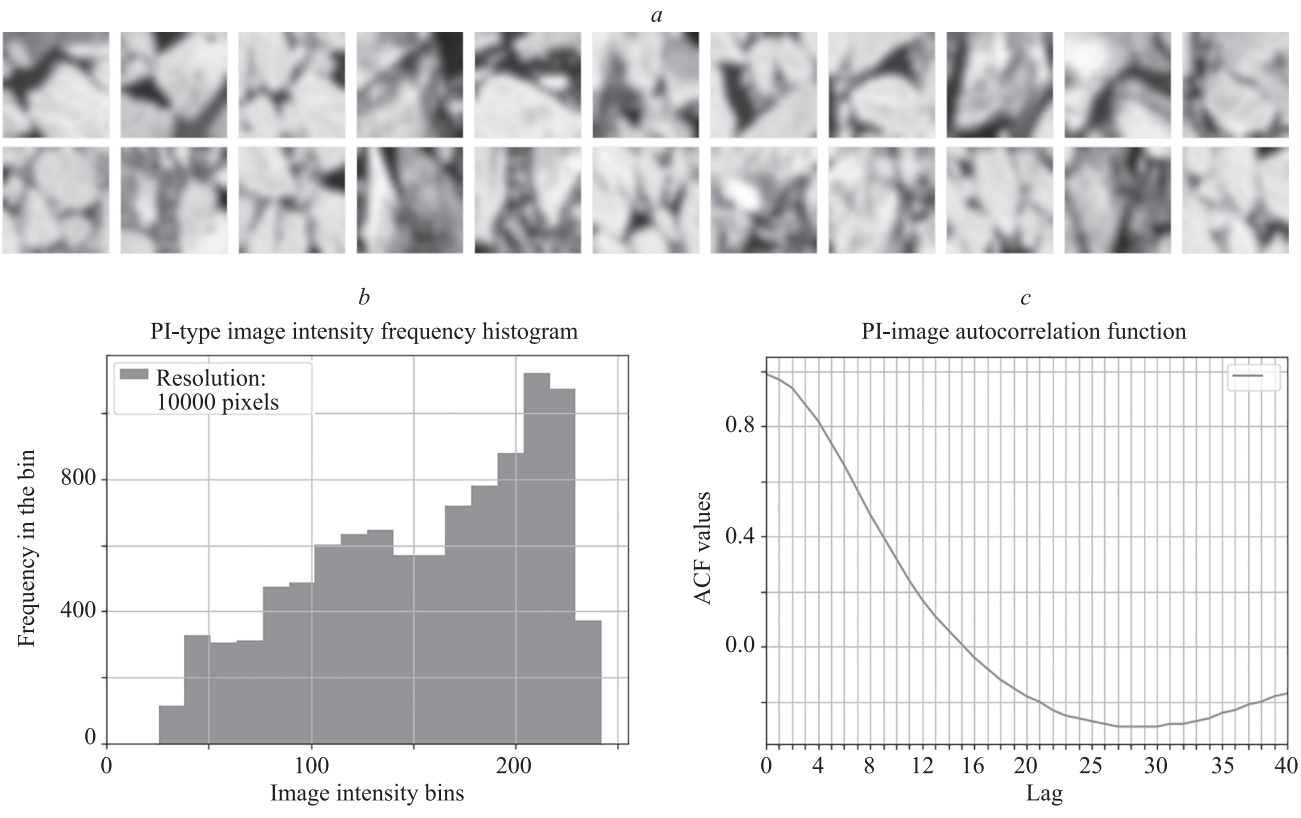

Fig. 4. Class “Pack Ice” (PI). Typical sample images from the PI-class (*a*). Intensity histogram plotted over the entire typical image from the PI-class (*b*). Typical autocorrelation function of PI-image (averaged over different slices) (*c*)

Table 1. The basic metrics values on the test Data Set

Image Class	Method	Precision	recall	f1-score	Support
Open Space (OS)	MC-SVM	1.00	0.96	0.98	24
	Resnet20	0.96	1.00	0.98	24
Marginal Ice Zone (MIZ)	MC-SVM	0.96	1.00	0.98	24
	Resnet20	0.92	1.00	0.96	24
Pack Ice (PI)	MC-SVM	1.00	1.00	1.00	43
	Resnet20	1.00	0.93	0.96	43

Table 2. Confusion matrices for ResNet 20 and MC-SVM

Image Class	Method	OS	MIZ	PI
Open Space (OS)	MC-SVM	23	0	1
	ResNet20	24	0	0
Marginal Ice Zone (MIZ)	MC-SVM	0	24	0
	ResNet20	0	24	0
Pack Ice (PI)	MC-SVM	0	0	42
	ResNet20	1	2	40

Test results

The results of the numerical studies are summarized in Tables 1, 2. The main information is contained in Table 1. Here we accumulate the results which were shown on the test Data Set by classifiers based on MC-SVM and Resnet20. A standard set of metrics was used to evaluate the classification results: precision, recall, and f1-score. The table shows that in the experiments exactly 24 samples from each class were used at the test stage.

Table 2 contains the so-called confusion matrix for classifier implementations by MC-SVM and Resnet20 schemes, respectively. In general, the classification results are quite good. A more detailed analysis of the results is given in the Discussion section.

Discussion

As follows from Tables 1, 2, the classifiers built according to different schemes, taking into account the low power of the Data Set, showed very decent results. At the same time, the classifier based on MC SVM is slightly superior in all parameters to the classifier based on ResNet20. This is due to the insufficient power of the Data Set to provide full training of the DL-classifier, ResNet20 in this case. It is known that the training of DL-classifiers, for example based on Deep Convolutional Neural Network, requires a Data Set of considerable power (more than 1000 instances for each class). This is due to the fact that DL-classifier is a very complex model which depends on tens of thousands (and more) parameters. From machine learning theory [29] follows that model complexity should grow "slowly" as the size of the training Data Set increases. Therefore, on small Data Sets, the DL-classifier simply does not have time to be trained due to the mismatch in the complexity of the classifier and the Data Set. Analysis of confusion matrixes shows that MC SVM made only 1 mistake, confusing classes PI and OO. This is probably due to the fact that these classes, despite their numerous differences, have common features: a significant part of the surface, in both cases, may occupy a coherent, texturally homogeneous array, for example, a water surface (OO-class) or a solid ice slab (PI-class). The ResNet20-based classifier made three errors. All errors are related to incorrect classification of samples from the PI-class. The reason for the errors: insufficient capacity of the Data Set to fully train the ResNet20-based classifier.

Conclusions

The paper suggests a new method for classifying the sea-ice floe size distribution type based on the use of low-quality video footage. Low quality of video footage is quite typical for high latitude conditions where most of the year a set of complex meteorological factors negatively affects the quality of aerial photography. That is why ice reconnaissance data processing should be able to compensate the negative influence of meteorological factors on the quality of ice surface imagery. In other words, ice reconnaissance data processing should be able to estimate with high reliability the sea-ice floe size distribution type because this estimation is one of the main results of ice reconnaissance. The sea-ice floe size distribution type classification method proposed in the article has high robustness to noises and distortions of the source video material which makes it an effective means of overcoming the negative influence of a complex high latitude meteorological environment. The simulation results showed high reliability in solving the task of estimating the sea-ice floe size distribution type which the proposed method provides under the condition of highly noisy and distorted source data. The proposed method is economical in the computational sense and, therefore, it can be implemented in software on a medium- and low-power computing platform placed on board a small-sized ice reconnaissance UAV.

References

1. Pershin N.V. Rational creation of navigation routes taking into account hydrometeorological conditions. *Proceedings of the Russian State Hydrometeorological University*, 2018, vol. 52, pp. 61–66. (in Russian)
2. Mironenko A.A. The Gradient Model of the Programmed Vessels Movement. *Navigation and Hydrography*, 2012, vol. 34, pp. 35–42. (in Russian)
3. Kalinina N.V. Influence of the ice navigation characteristics on the ice-breaker performance. *Transport Systems*, 2017, vol. 3(6), pp. 37–44. (in Russian). https://doi.org/10.46960/62045_2017_3_37
4. Horvat C., Tziperman E. The evolution of scaling laws in the sea ice floe size distribution. *Journal of Geophysical Research: Oceans*, 2017, vol. 122, no. 9, pp. 7630–7650. https://doi.org/10.1002/2016JC012573
5. Rothrock D., Thorndike A. Measuring the sea ice floe size distribution. *Journal of Geophysical Research*, 1984, vol. 89, no. C4, pp. 6477–6486. https://doi.org/10.1029/JC089iC04p06477
6. Alberello A., Onorato M., Bennetts L., Vichi M., Eayrs C., MacHutchon K., Toffoli A. Brief communication: Pancake ice floe size distribution during the winter expansion of the Antarctic marginal ice zone. *Cryosphere*, 2019, vol. 13, no. 1, pp. 41–48. https://doi.org/10.5194/tc-13-41-2019
7. Zhang J., Schweiger A., Steele M., Stern H. Sea ice floe size distribution in the marginal ice zone: Theory and numerical experiments. *Journal of Geophysical Research: Oceans*, 2015, vol. 120, no. 5, pp. 3484–3498. https://doi.org/10.1002/2015jc010770
8. Lu P., Li Z.J., Zhang Z.H., Dong X.L. Aerial observations of floe size distribution in the marginal ice zone of summer Prydz Bay. *Journal of Geophysical Research: Oceans*, 2008, vol. 113, no. 2, pp. C02011. https://doi.org/10.1029/2006jc003965
9. Toyota T., Takatsuji S., Nakayama M. Characteristics of sea ice floe size distribution in the seasonal ice zone. *Geophysical Research Letters*, 2006, vol. 33, no. 2, pp. L02616. https://doi.org/10.1029/2005gl024556
10. Toyota T., Haas C., Tamura T. Size distribution and shape properties of relatively small sea-ice floes in the Antarctic marginal ice zone in late winter. *Deep-Sea Research Part II: Topical Studies in Oceanography*, 2011, vol. 58, no. 9-10, pp. 1182–1193. https://doi.org/10.1016/j.dsr2.2010.10.034
11. Stern H.L., Schweiger A.J., Zhang J., Steele M. On reconciling disparate studies of the sea-ice floe size distribution. *Elementa*, 2018, vol. 6, pp. 49. https://doi.org/doi.org/10.1525/elementa.304
12. *Nautical Encyclopedic Reference Book*. V. 2. Ed. by N. Isanin. Leningrad, Sudostroenie Publ., 1987, 520 c. (in Russia)
13. Leshkevich G.A. Machine classification of freshwater ice types from Landsat — I digital data using ice albedos as training sets. *Remote Sensing of Environment*, 1985, vol. 17, no. 3, pp. 251–263. https://doi.org/10.1016/0034-4257(85)90098-7
14. Leshkevich G.A., Nghiem S.V. Satellite SAR remote sensing of Great Lakes ice cover, part 2. Ice classification and mapping. *Journal of Great Lakes Research*, 2007, vol. 33, no. 4, pp. 736–750. https://doi.org/10.3394/0380-1330(2007)33[736:SSRSOG]2.0.CO;2
15. Nghiem S.V., Leshkevich G.A. Satellite SAR remote sensing of Great Lakes ice cover, part 1. Ice backscatter signatures at C band. *Journal of Great Lakes Research*, 2007, vol. 33, no. 4, pp. 722–735. https://doi.org/10.3394/0380-1330(2007)33[722:SSRSOG]2.0.CO;2
16. Nghiem S.V., Leshkevich G.A. Advancing a satellite synthetic aperture radar (SAR) ice classification algorithm. *54th Annual Conference on Great Lakes Research. International Association for Great Lakes Research: Abstract Book*, 2011, pp. 181.
17. Schertler R.J., Mueller R.A., Jirberg R.J., Cooper D.W., Heighway J.E., Holmes A.D., Gedney R.T., Mark H. *Great Lakes All-weather Ice Information System: NASA Technical Memorandum NASA TM X-71815*.1975.
18. Leshkevich G., Nghiem S.V. Great Lakes ice classification using satellite C-band SAR multi-polarization data. *Journal of Great Lakes Research*, 2013, vol. 39, pp. 55–64. https://doi.org/10.1016/j.jglr.2013.05.003
19. Kamangir H., Rahnemoonfar M., Dobbs D., John Paden D., Fox G. *Detecting ice layers in radar images with deep learning,* 2018.
20. Birnbaum G., Lüpkes C. A new parameterization of surface drag in the marginal sea ice zone. *Tellus, Series A: Dynamic Meteorology and Oceanography*, 2002, vol. 54, no. 1, pp. 107–123. https://doi.org/10.3402/tellusa.v54i1.12121

Литература

1. Першин Н.В. Рациональное построение маршрутов плавания с учетом гидрометеорологических условий // Ученые записки Российского государственного гидрометеорологического университета. 2018. Т. 52. С. 61–66.
2. Мироненко А.А. Градиентная модель программного движения судна // Навигация и гидрография. 2012. Т. 34. С. 35–42.
3. Калинина Н.В. Влияние навигационных характеристик льда на ходкость ледокола // Транспортные системы. 2017. № 3(6). С. 37–44. https://doi.org/10.46960/62045_2017_3_37
4. Horvat C., Tziperman E. The evolution of scaling laws in the sea ice floe size distribution // Journal of Geophysical Research: Oceans. 2017. V. 122. N 9. P. 7630–7650. https://doi.org/10.1002/2016JC012573
5. Rothrock D., Thorndike A. Measuring the sea ice floe size distribution // Journal of Geophysical Research. 1984. V. 89. N C4. P. 6477–6486. https://doi.org/10.1029/JC089iC04p06477
6. Alberello A., Onorato M., Bennetts L., Vichi M., Eayrs C., MacHutchon K., Toffoli A. Brief communication: Pancake ice floe size distribution during the winter expansion of the Antarctic marginal ice zone // Cryosphere. 2019. V. 13. N 1. P. 41–48. https://doi.org/10.5194/tc-13-41-2019
7. Zhang J., Schweiger A., Steele M., Stern H. Sea ice floe size distribution in the marginal ice zone: Theory and numerical experiments // Journal of Geophysical Research: Oceans. 2015. V. 120. N 5. P. 3484–3498. https://doi.org/10.1002/2015jc010770
8. Lu P., Li Z.J., Zhang Z.H., Dong X.L. Aerial observations of floe size distribution in the marginal ice zone of summer Prydz Bay // Journal of Geophysical Research: Oceans. 2008. V. 113. N 2. P. C02011. https://doi.org/10.1029/2006jc003965
9. Toyota T., Takatsuji S., Nakayama M. Characteristics of sea ice floe size distribution in the seasonal ice zone // Geophysical Research Letters. 2006. V. 33. N 2. P. L02616. https://doi.org/10.1029/2005gl024556
10. Toyota T., Haas C., Tamura T. Size distribution and shape properties of relatively small sea-ice floes in the Antarctic marginal ice zone in late winter // Deep-Sea Research Part II: Topical Studies in Oceanography. 2011. V. 58. N 9-10. P. 1182–1193. https://doi.org/10.1016/j.dsr2.2010.10.034
11. Stern H.L., Schweiger A.J., Zhang J., Steele M. On reconciling disparate studies of the sea-ice floe size distribution // Elementa. 2018. V. 6. P. 49. https://doi.org/doi.org/10.1525/elementa.304
12. Морской энциклопедический справочник. Т. 2 / под ред. Н.Н. Исанина. Ленинград: Судостроение, 1987. 520 с.
13. Leshkevich G.A. Machine classification of freshwater ice types from Landsat - I digital data using ice albedos as training sets // Remote Sensing of Environment. 1985. V. 17. N 3. P. 251–263. https://doi.org/10.1016/0034-4257(85)90098-7
14. Leshkevich G.A., Nghiem S.V. Satellite SAR remote sensing of Great Lakes ice cover, part 2. Ice classification and mapping // Journal of Great Lakes Research. 2007. V. 33. N 4. P. 736–750. https://doi.org/10.3394/0380-1330(2007)33[736:SSRSOG]2.0.CO;2
15. Nghiem S.V., Leshkevich G.A. Satellite SAR remote sensing of Great Lakes ice cover, part 1. Ice backscatter signatures at C band // Journal of Great Lakes Research. 2007. V. 33. N 4. P. 722–735. https://doi.org/10.3394/0380-1330(2007)33[722:SSRSOG]2.0.CO;2
16. Nghiem S.V., Leshkevich G.A. Advancing a satellite synthetic aperture radar (SAR) ice classification algorithm // 54th Annual Conference on Great Lakes Research. International Association for Great Lakes Research: Abstract Book. 2011. P. 181.
17. Schertler R.J., Mueller R.A., Jirberg R.J., Cooper D.W., Heighway J.E., Holmes A.D., Gedney R.T., Mark H. Great Lakes All-weather Ice Information System: NASA Technical Memorandum NASA TM X-71815.1975.
18. Leshkevich G., Nghiem S.V. Great Lakes ice classification using satellite C-band SAR multi-polarization data // Journal of Great Lakes Research. 2013. V. 39. P. 55–64. https://doi.org/10.1016/j.jglr.2013.05.003
19. Kamangir H., Rahnemoonfar M., Dobbs D., John Paden D., Fox G. Detecting ice layers in radar images with deep learning. 2018.
20. Birnbaum G., Lüpkes C. A new parameterization of surface drag in the marginal sea ice zone // Tellus, Series A: Dynamic Meteorology and Oceanography. 2002. V. 54. N 1. P. 107–123. https://doi.org/10.3402/tellusa.v54i1.12121
21. Zhang Q., Skjetne R. Image processing for identification of sea-ice floes and the floe size distributions // IEEE Transactions on

21. Zhang Q., Skjetne R. Image processing for identification of sea-ice floes and the floe size distributions. *IEEE Transactions on Geoscience and Remote Sensing*, 2015, vol. 53, no. 5, pp. 2913–2924. https://doi.org/10.1109/tgrs.2014.2366640
22. Smith D., Barrett E., Scott J. Sea-ice type classification from ERS-1 SAR data based on grey level and texture information. *Polar Record*, 1995, vol. 31, no. 177, pp. 135–146. https://doi.org/10.1017/S0032247400013632
23. Shen X., Zhang J., Meng J., Zhang J., Ke C. Sea ice type classification based on random forest machine learning with Cryosat-2 altimeter data. *Proc. of the International Workshop on Remote Sensing with Intelligent Processing (RSIP)*, 2017, pp. 7958792. https://doi.org/10.1109/rsip.2017.7958792
24. Aksenov Y., Bateson A.W., Feltham D.L., Schröder D., Hosekova L., Ridley J.K., Impact of sea ice floe size distribution on seasonal fragmentation and melt of Arctic sea ice. *Cryosphere*, 2020, vol. 14, no. 2, pp. 403–428. https://doi.org/10.5194/tc-14-403-2020
25. Johannessen O.M., Bobylev L.P., Shalina E.V., Sandven S. Sea Ice in the Arctic: Past, Present and Future. *Springer Polar Sciences*, 2020, X, 575 p. https://doi.org/10.1007/978-3-030-21301-5
26. Timofeev A.V. Detection of a small target object in blurry images affected by affine distortions. *Scientific and Technical Journal of Information Technologies, Mechanics and Optics*, 2021, vol. 21, no. 2, pp. 206–224 (in Russian). https://doi.org/10.17586/2226-1494-2021-21-2-206-224
27. Cristianini N., Shawe-Taylor J. *An Introduction to Support Vector Machines and Other Kernel-based Learning Methods.* Cambridge University Press, 2000. https://doi.org/10.1017/CBO9780511801389
28. He K., Zhang X., Ren S., Sun J. Deep residual learning for image recognition. *Proc. of the 29th IEEE Conference on Computer Vision and Pattern Recognition (CVPR)*, 2016, pp. 770–778. https://doi.org/10.1109/cvpr.2016.90
29. Hastie T., Tibshirani R., Friedman J. *The Elements of Statistical Learning: Data Mining, Inference and Prediction*. Springer, 2009, XXII, 745 p. https://doi.org/10.1007/978-0-387-84858-7

Geoscience and Remote Sensing. 2015. V. 53. N 5. P. 2913–2924. https://doi.org/10.1109/tgrs.2014.2366640
22. Smith D., Barrett E., Scott J. Sea-ice type classification from ERS-1 SAR data based on grey level and texture information // Polar Record. 1995. V. 31. N 177. P. 135–146. https://doi.org/10.1017/S0032247400013632
23. Shen X., Zhang J., Meng J., Zhang J., Ke C. Sea ice type classification based on random forest machine learning with Cryosat-2 altimeter data // Proc. of the International Workshop on Remote Sensing with Intelligent Processing (RSIP). 2017. P. 7958792. https://doi.org/10.1109/rsip.2017.7958792
24. Aksenov Y., Bateson A.W., Feltham D.L., Schröder D., Hosekova L., Ridley J.K., Impact of sea ice floe size distribution on seasonal fragmentation and melt of Arctic sea ice // Cryosphere. 2020. V. 14. N 2. P. 403–428. https://doi.org/10.5194/tc-14-403-2020
25. Johannessen O.M., Bobylev L.P., Shalina E.V., Sandven S. Sea Ice in the Arctic: Past, Present and Future. Springer Polar Sciences, 2020. X, 575 p. https://doi.org/10.1007/978-3-030-21301-5
26. Тимофеев А.В. Инвариантный к линейным конформным преобразованиям алгоритм обнаружения размытого изображения целевого объекта малого размера // Научно-технический вестник информационных технологий, механики и оптики. 2021. Т. 2. № 2. С. 206–224. https://doi.org/10.17586/2226-1494-2021-21-2-206-224
27. Cristianini N., Shawe-Taylor J. An Introduction to Support Vector Machines and Other Kernel-based Learning Methods. Cambridge University Press, 2000. https://doi.org/10.1017/CBO9780511801389
28. He K., Zhang X., Ren S., Sun J. Deep residual learning for image recognition // Proc. of the 29th IEEE Conference on Computer Vision and Pattern Recognition (CVPR). 2016. P. 770–778. https://doi.org/10.1109/cvpr.2016.90
29. Hastie T., Tibshirani R., Friedman J. The Elements of Statistical Learning: Data Mining, Inference and Prediction. Springer, 2009. XXII, 745 p. https://doi.org/10.1007/978-0-387-84858-7

Authors

Andrey V. Timofeev — D. Sc., CSO, LLP "EqualiZoom", Astana, 010000, Kazakhstan, SC 56689367600, https://orcid.org/0000-0001-7212-5230, timofeev.andrey@gmail.com

Denis I. Groznov — Software Developer, LLP "EqualiZoom", Astana, 010000, Kazakhstan, SC 57218385022, https://orcid.org/0000-0002-7874-7118, d.i.groznov@yandex.ru

Received 20.07.2022
Approved after reviewing 10.08.2022
Accepted 27.09.2022

Авторы

Тимофеев Андрей Владимирович — доктор технических наук, научный директор, ТОО «Эквалайзум», Астана, 010000, Казахстан, SC 56689367600, https://orcid.org/0000-0001-7212-5230, timofeev.andrey@gmail.com

Грознов Денис Игоревич — разработчик, ТОО «Эквалайзум», Астана, 010000, Казахстан, SC 57218385022, https://orcid.org/0000-0002-7874-7118, d.i.groznov@yandex.ru

Статья поступила в редакцию 20.07.2022
Одобрена после рецензирования 10.08.2022
Принята к печати 27.09.2022